



# WEDNESDAY SLIDE CONFERENCE 2024-2025

Conference #12

06 November 2024

## CASE I:

### **Signalment:**

5-month-old, female intact, Domestic Short-hair, *Felis catus*, cat.

### **History:**

The patient presented to the referring veterinarian at 3 months of age for a 1 month history of abdominal distention which worsened post-prandially. Approximately 45 mL of yellow fluid was removed from the abdomen at this time. The patient was then referred to Colorado State University Veterinary Teaching Hospital for further work up: serum biochemistry demonstrated elevated liver enzymes and hyperbilirubinemia. Abdominal ultrasound showed severe intrahepatic biliary tract dilatation with no identifiable gallbladder, and 300 mL of a similar abdominal fluid was removed. Top differentials included a ductal plate malformation or other congenital malformations. The patient continued to decline despite medical management (Ursodiol and Spironolactone) and was humanely euthanized 1 month later.

### **Gross Pathology:**

On postmortem examination, there was moderate icterus and musculature atrophy. There was approximately 1300 mL of serous, yellow-green fluid in the abdominal cavity. The liver was yellow-to-green tinged and markedly enlarged with distorted, rounded lobes. There was serosal thickening with adhesions



**Figure 1-1. Presentation, kitten. 1300 cc of fluid were present in the abdomen at autopsy. (Photo courtesy of: Colorado State University Veterinary Diagnostic Laboratory, <https://vetmedbiosci.colostate.edu/vdl/>)**

from the liver to the diaphragm and stomach and there was no identifiable gall bladder. On cut section, the yellow to green discoloration was present throughout the parenchyma and there were numerous, tortuous, markedly dilated bile ducts filled with dark green fluid. The left lobe of the pancreas was edematous, nodular and irregular and markedly decreased in size with adhesions to the stomach. The spleen was very small, rounded and adhered to the stomach. The mesentery of the greater curvature of the stomach had prominent, slightly tortuous vasculature and was expanded by green-tinged edema.

### **Laboratory Results:**

#### Chemistry:

Phosphorus	7.0 mg/dL	(3.0 - 6.0)
Total Protein	6.2 g/dL	(6.3 - 8.0)
CK	828 IU/L	(60 - 350)

T-Bilirubin	1.6 mg/dL	(0.0 - 0.1)
ALP	392 IU/L	(10 – 80)
ALT	893 IU/L	(30 – 140)
AST	275 IU/L	(15 – 45)
GGT	22 IU/L	(0 - 0.5)
Sodium	154 mEQ/L	(149 – 157)
Potassium	6.12 mEQ/L	(3.7 - 5.4)
Chloride	116.6 mEQ/L	(115 – 125)
Bicarb	16.3 mEQ/L	(13 – 22)
Anion Gap	27 mmol/L	(16 – 26)
Calc Osmolality	317 mOsm/Kg	
Lipemia	20	(0 – 50)
Hemolysis	99	(0 – 50)
Icterus	2	(0 – 1)

Urinalysis:

U-Protein/Create	0.54 Ratio	(0.0-0.19)
Urine Protein	2+	
Urine Bilirubin	1+	
Urine pH	6	

Abdominal Fluid Analysis & Cytology:

Fluid Color	Yellow
Fluid Clarity	Cloudy
NCC Fld	700#/uL
RBC Fld	<10000 #/uL
Fluid PCV	0
Refr Protein Est	3.0 g/dL
Neutrophils #	399 #/uL
Neutrophils %	57%
Large Mononuclear #	287 #/uL
Large Mononuclear %	41%
Lymphocytes #	14 #/uL
Lymphocytes %	2%

**Microscopic Description:**

The liver capsule is thickened by variably mature fibrous to myxomatous connective tissue up to 0.6 mm thick with few regularly spaced vessels. Within the adjacent hepatic parenchyma, there are markedly dilated biliary profiles with thickened fibrous capsules. Cystic biliary spaces are lined by elongated and branching villi of biliary epithelium. Within the lumen there is a homogenous basophilic to amphophilic occasionally wispy to vacuolated material. Portal regions are diffusely surrounded by fibrous stroma which bridges between portal regions and entraps islands of



**Figure 1-2. Liver, kitten. The liver was yellow-to-green tinged and markedly enlarged with distorted, rounded lobes. (Photo courtesy of: Colorado State University Veterinary Diagnostic Laboratory, <https://vetmed-biosci.colostate.edu/vdl/>)**

hepatocytes. Associated with portal tracts and fibrosis, there are abundant torturous biliary profiles with oval cell hyperplasia and arteriolar reduplication. Portal veins are often small and there is variable lymphatic dilation. Mild infiltrates of neutrophils with fewer lymphocytes, plasma cells and Kupffer cells dissect portal regions. There is increased connective tissue surrounding central veins and multifocal mild sinusoidal dilation.

Masson’s Trichrome Histochemistry:

Liver: Trichrome staining demonstrates marked fibrosis surrounding dilated biliary profiles, often entrapping islands of hepatocytes. There is a finer collagen network bridging remaining portal regions and surrounding central veins.

Cytokeratin 19 Immunohistochemistry:

Liver: There is moderate to strong immunoreactivity to cytokeratin 19 throughout cystic bile ducts and proliferative biliary epithelium within portal regions and extending between lobules. Occasionally, individual oval to



**Figure 1-3. Liver, kitten. On cut section, intrahepatic bile ducts are markedly ectatic and tortuous. (Photo courtesy of: Colorado State University Veterinary Diagnostic Laboratory, <https://vetmedbiosci.colostate.edu/vdl/>)**

spindloid cytokeratin 19-positive cells directly oppose periportal hepatocytes.

**Contributor’s Morphologic Diagnosis:**

Liver: Chronic marked bridging fibrosis with ductular reaction, arteriolar reduplication, portal vein hypoplasia and marked cystic dilation of bile ducts (Caroli’s disease); moderate central vein fibrosis.

**Contributor’s Comment:**

Physical exam, ultrasound, gross and histologic findings in this case are most suggestive of Caroli malformation/disease, which is a ductal plate malformation (DPM) characterized by congenital hepatic fibrosis and cystic bile ducts.<sup>1</sup>

DPMS are a group of developmental biliary disorders rarely reported in veterinary species.<sup>1</sup> In normal development, hepatoblasts are bipotent, capable of differentiating into biliary epithelium or periportal hepatocytes.

The fate of hepatoblasts is largely dependent on transcription factors. Hepatoblasts that give rise to biliary epithelium undergo tubulogenesis, forming a double layer of cuboidal cells surrounding a rudimentary portal vein. This coordinated series of events is orchestrated by TGF- $\beta$ , Notch, and Wnt signaling pathways, forming the embryonic ductal plate.<sup>7</sup> Hepatoblasts that do not undergo tubulogenesis either involute or differentiate into periportal hepatocytes.<sup>1,5-7</sup>

Malformations within the ductal plate arise when hepatoblasts do not undergo tubulogenesis and also fail to involute, resulting in persistent embryonic bile ducts. It is important to note that DPM encompasses a continuum of phenotypes which reflect the level at which the developing biliary tree is affected.<sup>1</sup> This spectrum includes Caroli malformation (presented in this case), biliary hamartomas (also referred to as von Meyenburg complexes), congenital hepatic fibrosis (CHF), and polycystic liver disease (PCLD).<sup>1,5</sup> In cases of Caroli malformation, disruption occurs at the level of segmental bile ducts (first branch of the hepatic duct), leading to large dilated/cystic persistent ducts.

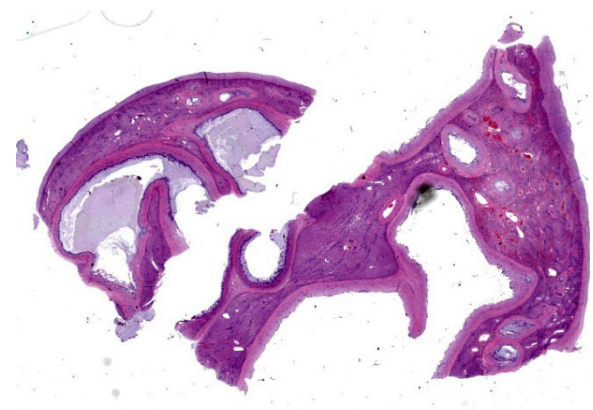


**Figure 1-4. Liver, kitten. There is bridging portal fibrosis entrapping markedly ectatic bile ducts (which measure up to 6mm in diameter). (HE, 5X)**

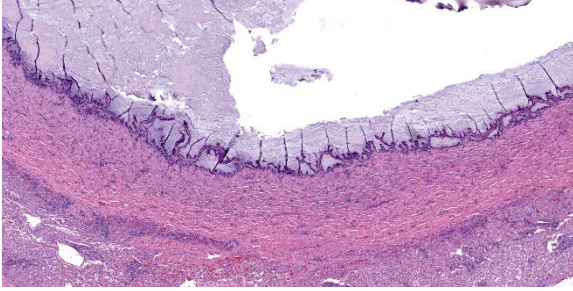


**Figure 1-5. Liver, kitten. Ectatic bile ducts are lined by hyperplastic epithelium and have a thick 1mm fibrous capsule. (HE, 44X)**

Few cases of DPMs have been reported in cats, including Caroli malformation with a portosystemic shunt,<sup>6</sup> congenital hepatic fibrosis<sup>8</sup> (see WSC 2019-2020, Conference 7, Case 1), bile duct hamartomas (see WSC 2021-2022, Conference 1, Case 4), and polycystic liver disease (often in combination with adult polycystic kidney disease).<sup>3,4</sup> One retrospective study characterized clinical findings in 30 boxer dogs diagnosed with DPMs.<sup>5</sup> In this study, the most common clinical feature was increased liver enzymes (n=28/30), followed by gastrointestinal signs (n=16/30), poor body condition (n=14/30), abdominal effusion (n=9/30), and hepatic encephalopathies (n=2/30); however, these changes are not unique to DPMs which can challenge clinical diagnoses. Such data is currently lacking in cats.

Gallbladder atresia has also been reported in dogs with DPMs.<sup>5</sup> In the presented case, the gall bladder was not identified with gross or histologic examination.

In cases of congenital hepatic fibrosis (CHF), histopathologic findings include bridging hepatic fibrosis, numerous irregular bile duct profiles, diminished or absent portal veins, and arteriolar reduplication. These histologic findings in addition to large, tortuous and cystic biliary ducts are termed Caroli malfor-

mation. DPMs lack nodular regeneration, cirrhosis, and cholangitis. Cytokeratin 19 (CK19) is expressed in hepatoblast precursor cells and committed biliary epithelium and can be used as a marker to confirm cellular histogenesis in these cases.<sup>1,5</sup>

Differential diagnoses include primary portal vein hypoplasia (PVHP), obstructive biliary disease, and lobular dissecting hepatic fibrosis (dogs only).

**Primary portal vein hypoplasia (PVHP):** In DPMs, intrahepatic presinusoid hypertension may redirect portal flow away from the liver, resulting in an acquired portosystemic shunt. Therefore, decreased/absent portal veins with arteriolar reduplication can overlap between DPMs and PVHPs; however, cases of a PVHP often lack marked biliary hyperplasia, biliary ectasia, and periportal fibrosis.<sup>1,2</sup>

**Obstructive biliary disease:** Similar to DPMs, obstructive biliary disease includes bile duct dilation and tortuosity; however, peribiliary fibrosis does not bridge portal regions, and the presence of periductal edema with inflammation are unique to obstructive biliary disease.<sup>5</sup>

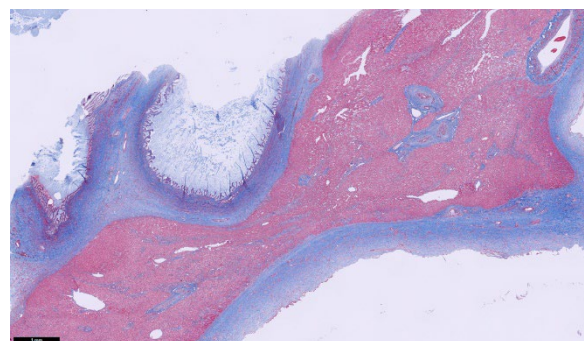


**Figure 1-6. Liver, kitten. A Masson's trichrome demonstrates the thickened capsule, fibrotic walls of ectatic bile ducts, and bridging portal fibrosis. (Masson's trichrome, 40X) (Photo courtesy of: Colorado State University Veterinary Diagnostic Laboratory, <https://vetmedbiosci.colostate.edu/vdl/>)**

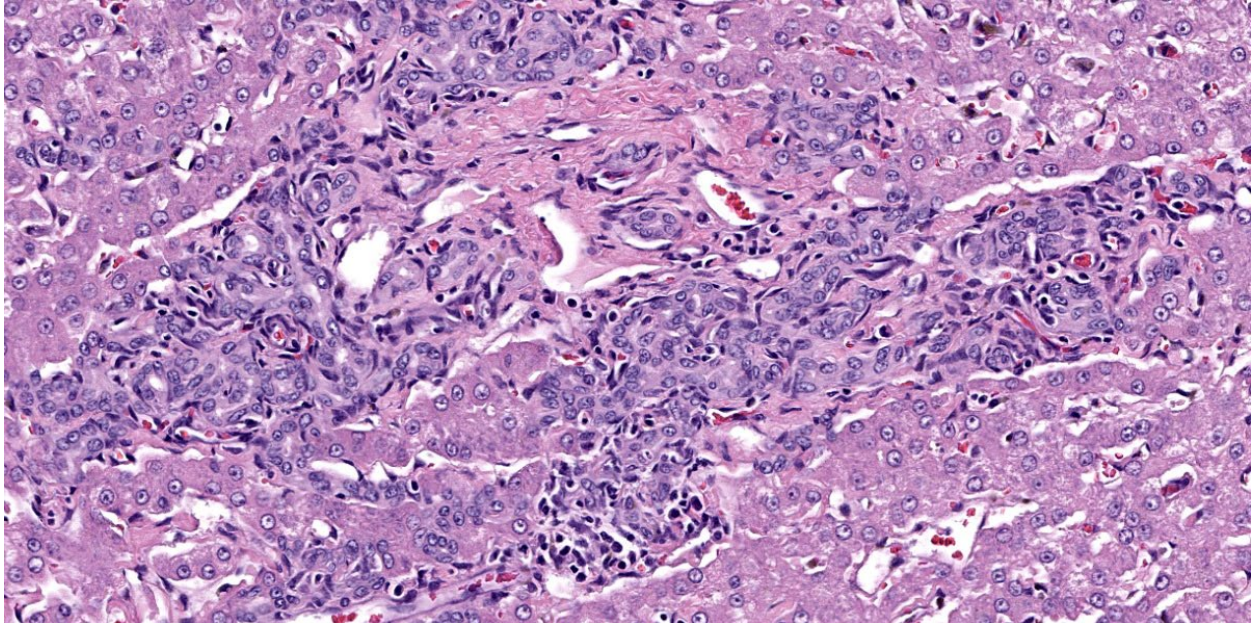


**Figure 1-7. Liver, kitten. There is marked biliary hyperplasia in areas of portal fibrosis. Portal areas contain numerous arteriolar profiles, but few discernible portal veins. (HE, 300X)**

Lobular dissecting hepatic fibrosis: Lobular dissecting hepatic fibrosis is often accompanied by nodular regeneration and cirrhosis, both of which are not features of DPMs.<sup>1,2</sup>

**Contributing Institution:**

Colorado State University Veterinary Diagnostic Laboratory

<https://vetmedbiosci.colostate.edu/vdl/>

**JPC Diagnosis:**

Liver: Ductal plate malformation.

**JPC Comment:**

This week's moderator was the renowned Dr. John Cullen who led participants through a liver-centric conference with 4 cases that emphasized careful review of the slide and taking a 'census' of liver features along the way.

The contributor provides an excellent summary of ductal plate malformations in this first case. Dr. Cullen ultimately agreed that

the features presented were likely consistent with Caroli's disease, though there were several important additional criteria to consider. Foremost, there was no evidence of obstruction and/or inflammation as an inciting cause for dilatation of the bile ducts which is an important rule out – this can be complicated as ascending infection often accompanies distension of the duct. That this cat was young (5 months) likely limited inflammation. In addition, as Caroli's disease affects the large ducts specifically. . Figure 1-3 is supportive on its own for Caroli's disease. Careful dissection of the entire liver with a good gross description is therefore advisable. Though a lack of a gallbladder is associated with DPMs resembling Caroli's disease in dogs, gallbladder agenesis has been rarely reported in this condition in cats.

Though the abnormal proliferation of biliary ductules in the fibrotic portal areas was an obvious feature of this case, the absence of portal vein profiles was a bit more subtle. Dr.

Cullen emphasized reviewing multiple portal tracts as part of his census and specifically locating the portal vein, hepatic artery, bile duct, and lymphatics and comparing both larger tracts and smaller tracts for features. The latter is important for considering the branch level of primary portal vein hypoplasia as only secondary branches may be hypoplastic. Additionally, the marked dilatation of bile ducts was a helpful feature for this case, though the diagnosis of DPM writ large does not require this if there is modest dilation concurrent with portal vein hypoplasia.

Finally, there are several ancillary features of this slide worth capturing. The thick hepatic capsule likely represents stretching of the liver and increased mechanical response. The marked dilatation of bile ducts increases interstitial pressure which in turn allowed for leakage of fibrinogen in lymph and eventual conversion to the mature collagen seen in section. The degree of fibrosis present with Masson's trichrome is notable (figure 1-6) as well, and indicates (in a very non-specific vernacular), impaired "cross-talk" between epithelial and mesenchymal tissues during intrahepatic biliary tree development. Material within the ductular lumen stained with Alcian blue (i.e. containing mucus), though ductular epithelial secretions are variable and include other constituents as well.

#### References:

1. Cullen JM, Stalker MJ. Liver and biliary system. In: Maxie MG, ed. *Jubb, Kennedy, and Palmer's Pathology of Domestic Animals*. 6th ed. Vol 2. Philadelphia, PA: Elsevier; 2016:264-267.
2. Cullen JM. Summary of the World Small Animal Veterinary Association standardization committee guide to classification of liver disease in dogs and cats. *Vet Clin North Am Small Anim Pract*. 2009 May;39(3):395-418.
3. Hirose N, Uchida K, Kanemoto H, et al. A retrospective histopathological survey on canine and feline liver diseases at the University of Tokyo between 2006 and 2012. *J Vet Med Sci*. 2014; 76: 1015–1020.
4. King EM, Pappano M, Lorbach SK, Green EM, Parker VJ, Schreeg ME. Severe polycystic liver disease in a cat. *Journal of Feline Medicine and Surgery Open Reports*. 2023;9(2).
5. Pillai S, Center SA, McDonough SP, et al. Ductal Plate Malformation in the Liver of Boxer Dogs: Clinical and Histological Features. *Vet Pathol*. 2016 May;53(3):602-13.
6. Roberts ML, Rine S, Lam A. Caroli's-type ductal plate malformation and a portosystemic shunt in a 4-month-old kitten. *JFMS Open Rep*. 2018 Nov 20;4(2):2055116918812329.
7. Wills ES, Roepman R, Drenth JP. Polycystic liver disease: ductal plate malformation and the primary cilium. *Trends Mol Med*. 2014; 20:261–270.
8. Zandyliet MM, Szatmári V, van den Ingh T, Rothuizen J. Acquired portosystemic shunting in 2 cats secondary to congenital hepatic fibrosis. *J Vet Intern Med*. 2005 Sep-Oct;19(5):765-7.

#### CASE II:

##### **Signalment:**

10-year-old, male neutered domestic cat, feline (*Felis silvestris catus*).

##### **History:**

This animal was referred to the veterinary clinic for weakness and abnormal vocalizations. At the clinical examination, severe pallor of the external mucosae, asthenia and peritoneal blood effusion were detected. Complete blood count and clinical chemistry



**Figure 2-1. Liver, cat. At subgross magnification, there is a retiform pattern of pallor in centrilobular areas. (HE, 5X)**

showed severe anemia and increased liver enzymes. On ultrasound examination the liver appeared moderately enlarged in size, with a coarse granular texture and slightly rounded margins. Liver biopsies were performed during laparotomy for histological examination.

### **Gross Pathology:**

At laparoscopy, it was referred that the liver appeared enlarged and on the surface there were multifocal dark-red lesions continuously draining blood (consistent with hemorrhages).

### **Laboratory Results:**

Complete blood count revealed many abnormal values, including WBC  $19,30 \times 10^3/\text{ul}$ , Reference Intervals (RI) 5,00-11,00); RBC  $4,65 \times 10^6/\text{ul}$  (RI 5,00-10,00); MCH 17,80 pg (RI 12,50-17,50); MCHC 36,90 g/dl (RI 29,00-36,00); RDW 22,70 % (RI 13,00-17,00); HCT 22,50 % (RI 24,00-45,00); lymphocytes 8,40 % (RI 20,00-55,00); monocytes 5,10 % (RI 1,00-4,00); eosinophils 17,50 % (RI 0,00-12,00); MPV 10,00 fl (RI 12,00-17,00). Clinical chemistry showed creatine kinase 928,50 U/l (RI < 250,00); AST 94 U/l (RI 0 – 57); cholesterol 251,90 mg/dl (RI 56 – 241,00), glucose 34,27 mg/dl (RI 61 – 155,00); BUN 12 mg/dl (RI 13 – 31); iron 76,77 ug/dL (RI 110,00 - 169,00).

### **Microscopic Description:**

Liver: approximately 70% of the liver parenchyma is affected by multifocal to coalescing

areas of moderate to marked sinusoidal dilatation of variable dimensions, irregular in shape and randomly distributed. Occasionally in these areas, loss of endothelial demarcation is evident. Admixed with the dilated sinusoids and lacunae there are extravascular erythrocytes (hemorrhages), meshwork of eosinophilic, amorphous and fibrillar material (fibrin and necrotic debris), few cytoplasmic and nuclear fragments of hepatocytes (hepatocytes necrosis and loss) and rare neutrophils characterized by variable pyknosis, karyolysis and karyorrhexis. In unaffected areas the hepatocellular cords are irregularly distributed and there is loss of lobular architecture. Immediately adjacent to these areas the hepatocytes show mild to moderate atrophy. In the rest of the section, the hepatocyte cords show irregular radial organization and mild thickening (2-3 layers) and hepatocytes are diffusely characterized by large cytoplasm containing mild to moderate amounts of optically empty microvacuoles (vacuolar degeneration with mild steatosis). The hepatocytes show frequent binucleation and occasional mitoses (hyperplasia). Furthermore, multifocally the blood lacunae extend to the subsurface and here the hepatic capsule is covered by a small amount of fibrin mixed with scant extravascular erythrocytes. Small hemorrhages are evident diffusely in the subcapsular-capsular tissue. In addition, multifocally there is a mild hyperplasia of the lining mesothelium which is occasionally is distributed over two layers.

### **Contributor's Morphologic Diagnosis:**

Liver: Sinusoidal lacunae (blood-filled), multifocal to coalescing and random, moderate with heptacellular necrosis, loss, and atrophy with multifocal mild fibrinous perihepatitis, hemorrhage, and multifocal mild mesothelial hyperplasia.

### **Contributor's Comment:**

This case represents an unusual lesion that was not matching any specific entity. One

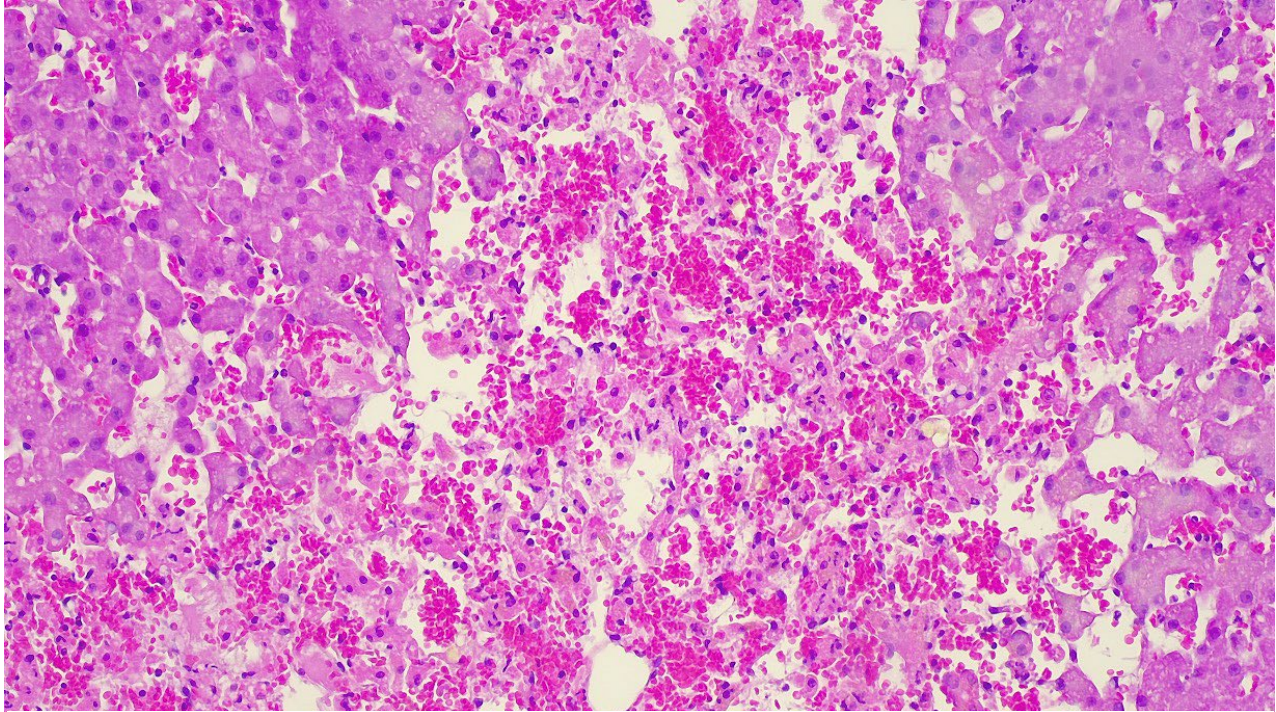
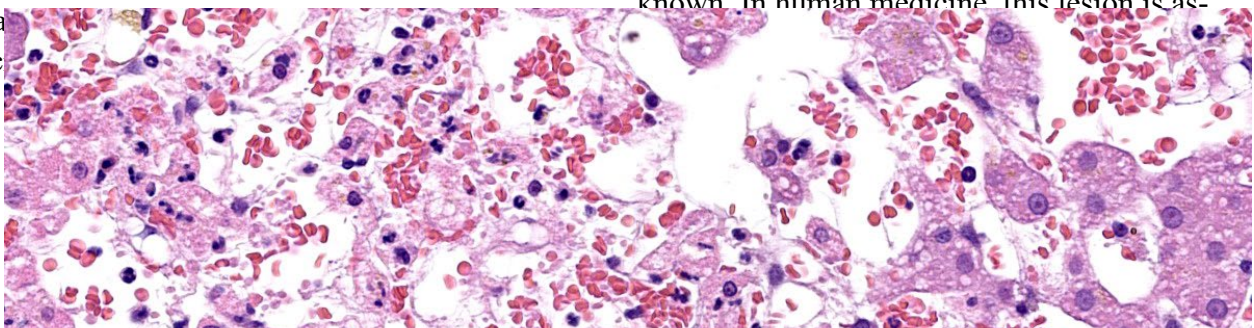


**Figure 2-2. Liver, cat. Within dilated sinusoids, there is abundant hemorrhage, fibrin and necrotic debris, few cytoplasmic and nuclear fragments of hepatocytes (hepatocyte necrosis and loss) and viable and necrotic neutrophils (HE, 200X) (Photo courtesy of: Department of Comparative Biomedicine and Food Science, Viale dell'Università 15, 35020, Legnaro (PD), Italy; <https://www.bca.unipd.it/>)**

disease that was discussed as possible part of the diagnosis was hepatitis peliosis which is what this case was submitted as.

Hepatitis peliosis is an uncommon condition of the liver characterized by the presence of numerous blood-filled cystic spaces. These cystic spaces may be lined by endothelial cells (phlebotatic form), therefore indicating sinusoidal dilatation associated also with reticulin alterations.<sup>6</sup> Conversely, in the parenchymal form the cystic spaces are formed by necrosis of the hepatocytes and endothelial lining that can therefore be absent multifocally.<sup>6</sup> In both cases, grossly, the lesions are characterized by multifocal dark-red areas,

va  
sc



perforial severe bleeding is usually not described.

In our case, a parenchymal form was considered as more suitable because of the detected necrosis.

Usually, hepatitis peliosis is not associated with clinical alterations linked to liver dysfunction, whereas in our case an increase in liver enzymes and anemia were observed. For this reason, a primary necrotizing hepatitis with unusual and marked cystic sinusoidal dilatation could not be ruled out as a diagnosis.

Hepatitis peliosis has been reported in cattle,<sup>11</sup> dogs,<sup>8,12</sup> and cats.<sup>3</sup> Its pathogenesis is still unknown. In human medicine this lesion is as-



infections such as *Bartonella henselae* and *B. quintana*.<sup>1</sup> In humans and lab animals, increases in vascular endothelial growth factor (VEGF) have been implicated in lesion development.<sup>14</sup> In addition, *B. henselae* infection notably leads to activation of hypoxia-inducible factor-1 (HIF-1) which can induce a pro-angiogenic response in the host via VEGF and IL-8.<sup>10</sup> In dogs, hepatitis peliosis has been described in one case following diphenhydramine<sup>2</sup> intoxication and in another case with *B. henselae* infection.<sup>9</sup> In cats, this condition is relatively common in elderly subjects (particularly the phlebotactic form) and it seems that there is not a clear association with *B. henselae* infection.<sup>4</sup> In cattle, a specific form of hepatitis peliosis has been described in animals poisoned by *Pimelea* plants.<sup>13</sup>

In conclusion, this is an unusual case in which both necrosis and marked dilation of blood spaces (hepatitis peliosis-like lesions) were detected. No additional analysis for

infectious diseases or toxins were conducted for this case.

**Contributing Institution:**

Department of Comparative Biomedicine and Food Science, Viale

dell'Università 15, 35020, Legnaro (PD), Italy; <https://www.bca.unipd.it/>

**JPC Diagnosis:**

Liver: Sinusoidal dilation and hemorrhage, centrilobular, diffuse, severe, with hepatocellular atrophy and necrosis and multiple subcapsular hematomas.

**JPC Comment:**

We thank the contributor for submitting this interesting case. Many conference participants weren't initially sure what to make of the presentation, with the centrilobular to midzonal distribution of the necrosis leading some to consider a toxicant. We agree that hepatitis peliosis is an excellent differential for this case; however, under the careful eye (and

immense expertise) of Dr. Cullen, we were able to arrive at a slightly different diagnosis however.

As the contributor notes, the diagnosis of hepatitis peliosis involves disruption of the reticulin framework. Such changes were notably absent on our reticulin stain. In addition, Masson's trichrome highlighted centrilobular fibrosis which was suggestive of a more chronic lesion. Moreover, hepatitis peliosis changes should reflect a random distribution, whereas the distribution of necrosis in the submitted sections was repeatable and specific in this case. For these reasons, we do not favor the contributor's diagnosis and prefer a diagnosis of chronic sinusoidal outflow issues (i.e. dilation and congestion).<sup>15,16</sup>

An important ruleout for centrilobular necrosis is hypertension secondary to chronic passive congestion (right-sided heart failure), veno-occlusive disease, or thrombosis of the vena cava (e.g. Budd-Chiari syndrome).<sup>15,16</sup> Though the contributor did not report cardiac lesions in this cat, the hypereosinophilia noted on bloodwork is an interesting (if non-specific) finding that could hint a *Dirofilaria* infection – heartworm has been described in cats in northern Italy.<sup>7</sup> Thrombosis of the vena cava and veno-occlusive disease are both rare in cats.<sup>5</sup> Mechanistically, the progression of hepatocyte loss to fibrosis accentuates portal hypertension (and hypoxia) with subsequent atrophy and necrosis of remaining hepatocytes. An interesting ancillary feature of this case was numerous erythrocytes within the space of Disse. Conference participants felt that this likely reflected both endothelial damage and increased sinusoidal pressure. Erythrocyte extravasation may be encountered in cases with and without impairment of venous outflow however.<sup>15</sup>

Lastly, we briefly discussed the idea of a toxin in this case. There are several features that do not fit with acute intoxication, however. Histologically, atrophy, congestion, and fibrosis are not consistent with a single intoxicating event despite the presence of hepatocyte necrosis. The low AST on this cat's bloodwork also argues against this. Absent the other clinical data and history in this cat, a chronic intoxication with an acute disruption could present in this manner.

### References:

1. Ahsan N, Holman MJ, Riley TR et al. Peliosis hepatitis due to *Bartonella henselae* in transplantation: a hemato-hepato-renal syndrome. *Transplantation*. 1998;65(7):1000-1003.
2. Beal MW, Doherty AM, Curcio K. Peliosis hepatitis and hemoperitoneum in a dog with diphacinone intoxication. *Journal of Veterinary Emergency and Critical Care*. 2008;18(4):388-392.
3. Brown PJ, Henderson JP, Galloway P, O'Dair H, & Wyatt JM. Peliosis hepatitis and telangiectasis in 18 cats. *Journal of Small Animal Practice*. 1994;35(2):73-77.
4. Buchmann AU, Kempf VAJ, Kershaw O, Gruber AD. Peliosis hepatitis in cats is not associated with *Bartonella henselae* infections. *Veterinary Pathology*. 2010;47(1):163-166.
5. Cave TA, Martineau H, Dickie A, Thompson H, Argyle DJ. Idiopathic hepatic veno-occlusive disease causing Budd-Chiari-like syndrome in a cat. *J Small Anim Pract*. 2002 Sep;43(9):411-5.
6. Cullen JM, Stalker MJ. Liver and Biliary System. In: Maxie MG, ed. *Jubb, Kennedy & Palmer's Pathology of Domestic Animals*. Vol 2. 6th ed. St. Louis, MO: Elsevier; 2016:258-352.
7. Grillini M, et al. Evidence of *Dirofilaria immitis* in Felids in North-Eastern Italy.

- Pathogens*. 2022;11(10):1216.
8. Inoue S, Matsunuma N, Ono K, Hayashi T, Takahashi R, Goto N, Fujiwara K. Five cases of canine peliosis hepatis. *Nihon Juigaku Zasshi ((The Japanese Journal of Veterinary Science))*. 1988 Apr;50(2):565-7.
  9. Kitchell BE, Fan TM, Kordick D et al. Peliosis hepatis in a dog infected with *Bartonella henselae*. *Journal of the American Veterinary Medical Association*. 2000;216(4):519-523.
  10. Kempf VA, Lebidziejewski M, Alitalo K et al. Activation of hypoxia-inducible factor-1 in bacillary angiomatosis: evidence for a role of hypoxia-inducible factor-1 in bacterial infections. *Circulation*. 2005;111(8):1054-1062.
  11. Onda H, Kaneda Y, Ito Y, Wakabayashi T. Peliosis hepatis: a specific lesion in the bovine liver. *Acta Pathologica Japonica* 1982; 32(6), 1053-1058.
  12. Sapieryński R. Peliosis hepatis-like lesion in a pekingese dog. A case report. *Polish Journal of Veterinary Sciences*. 2007;10(1):43-46.
  13. Seawright AA. Phlebotatic peliosis hepatis in Australian cattle. *Veterinary and Human Toxicology*. 1984;26(3):208-213.
  14. Wong AK, Alfert M, Castrillon DH et al. Excessive tumor-elaborated VEGF and its neutralization define a lethal paraneoplastic syndrome. *Proceedings of the National Academy of Sciences*. 2001;98(13):7481-7486.
  15. Kakar S, Kamath PS, Burgart LJ. Sinusoidal dilatation and congestion in liver biopsy: is it always due to venous outflow impairment? *Arch Pathol Lab Med*. 2004 Aug;128(8):901-4.
  16. Kakar S, Batts KP, Poterucha JJ, Burgart LJ. Histologic changes mimicking biliary disease in liver biopsies with venous outflow impairment. *Mod Pathol*. 2004 Jul;17(7):874-8.

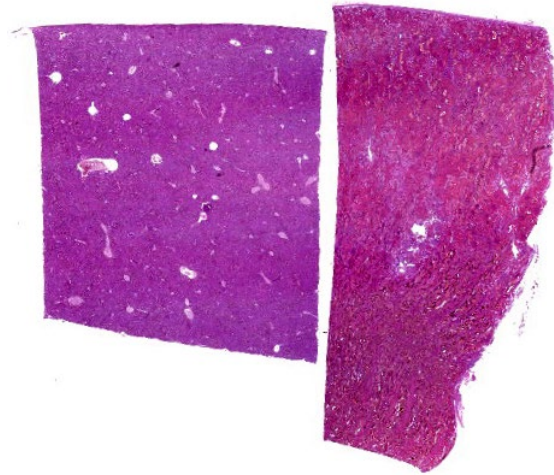


**Figure 3-1. Liver and kidney, sheep. Sections from these tissues are submitted for examination. (HE, 5X)**

### **CASE III:**

#### **Signalment:**

Adult pregnant Texel sheep (*Ovis aries*).

#### **History:**

12 of ~1,500 sheep exhibited acute depression, red urine (hemoglobinuria), yellow discoloration of the conjunctiva (jaundice), and died over a 10-month period. The sheep grazed on red clover and annual ryegrass, had access to foxtail millet and oat hay, and were supplemented with soybean meal, molasses, and slow-release urea. The flock was administered a multivalent vaccine to prevent clostridial diseases, as well as anthelmintic drugs.

#### **Gross Pathology:**

The subcutaneous tissue and the abdominal and pericardial fat were slightly icteric, and the carcass had a brownish hue (presumably due to methemoglobinemia). Bilaterally, the renal parenchyma involving both the cortex and medulla showed a diffuse dark red to black discoloration (hemoglobinuric nephrosis). The urinary bladder contained ~3 mL of dark red urine (hemoglobinuria). The liver

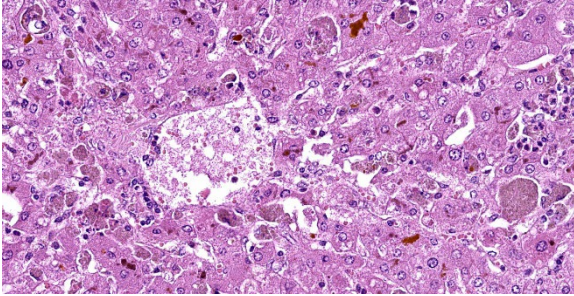


**Figure 3-2. Liver, sheep. There is diffuse necrosis of centrilobular hepatocytes. There is marked canalicular cholestasis as well.**

was diffusely tan. Additional changes included mild ecchymoses in the serosa of the small and large intestine, abundant pink stable froth in the lumen of the trachea, extra and intrapulmonary bronchi with diffuse pulmonary edema, and free dark, red-tinged fluid in the abdominal and thoracic cavities and pericardial sac (mild hydroperitoneum, hydrothorax and hydropericardium). Incidentally, there were multiple, white, spherical to ovoid, 7-9 mm in diameter, solid nodules in the esophageal muscular layer morphologically resembling *Sarcocystis gigantea* cysts, and a few adult nematodes compatible with *Trichuris* sp. in the lumen of the colon.

**Laboratory Results:**

No laboratory tests were performed before autopsy. Aerobic and microaerobic bacterial cultures from lung, liver, kidney, urine, and colon were unremarkable. PCR, qPCR and direct fluorescent antibody test for *Leptospira* spp. from liver, kidney, and urine were all negative. A heavy metal screen was performed in samples of liver and kidney with the following results:

Analyte	Liver	
	Result	Reference range
Lead	ND	<1
Manganese	1.8	2-4.4
Iron	400	30-300
Mercury	ND	<1
Arsenic	ND	<4
Molybdenum	ND	<6
Zinc	57	30-75
Copper	867	25-100*
Cadmium	ND	<2

Analyte	Kidney	
	Result	Reference range
Lead	ND	<1
Manganese	1.2	0.8-2.5
Iron	800	30-200
Mercury	ND	<1
Arsenic	ND	<1
Molybdenum	ND	<2
Zinc	43	20-40
Copper	207	4-5.5*
Cadmium	ND	<4

ND: not detected. All values are expressed in ppm on a wet-weight basis. \*>250 ppm in liver and >15 ppm in kidney is consistent with copper toxicity.

**Microscopic Description:**

Liver: hepatocytes throughout centrilobular and midzonal areas exhibit swelling, poorly defined cell boundaries, and vesicular nuclei (degeneration) or have shrunken hypereosinophilic cytoplasm with angular borders and pyknotic nucleus or karyorrhexis (necrosis). Occasionally, necrotic hepatocytes are surrounded by aggregates of neutrophils, macrophages and extravasated erythrocytes. Hepatic cords are distorted, and hepatocyte orientation is altered, especially around the centrilobular regions. Scattered in the parenchyma many hepatocytes and Kupffer cells contain cytoplasmic, finely granular, brownish to gray material (interpreted as copper). Multifocally, a golden to orange amorphous

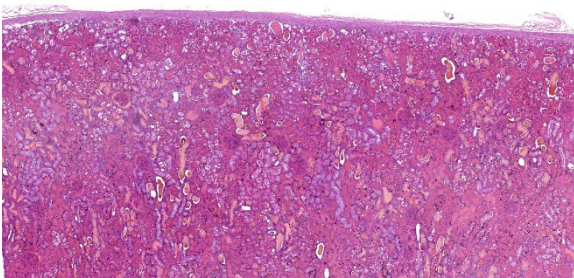


**Figure 3-3. Kidney, sheep. Normal tubular architecture is altered with tubular lumina filled with protein and hemorrhage. (HE, 33X)**

pigment plugs the canaliculi (cholestasis). Portal regions are multifocally infiltrated by moderate numbers of pigment-laden macrophages and fewer lymphocytes.

Kidney: diffusely, cortical and medullary tubules, and glomerular filtration spaces are ectatic, and contain eosinophilic proteinic material/droplets and hyaline casts (consistent with hemoglobin). Cortical tubular epithelial cells exhibit a wide variety of changes including foamy cytoplasm, tumefaction, nuclear swelling (degeneration), attenuation, or hyper eosinophilic cytoplasm with pyknosis (necrosis) frequently involving entire segments of the tubules (tubulorrhexis). Multifocally necrotic epithelial cells slough into the tubular lumen. Intracytoplasmic, coarse, granular, brown to black pigment (consistent with iron/hemosiderin) is widely distributed throughout the epithelium of the proximal tubules.

**Contributor’s Morphologic Diagnosis:**

1. Liver: Hepatocellular degeneration and necrosis, centrilobular to midzonal, acute, severe, diffuse, with intracytoplasmic granular material (consistent with copper) in Kupffer cells and hepatocytes, canalicular cholestasis, moderate, multifocal, neutrophilic and histiocytic hepatitis and portal hepatitis.

2. Kidney: Nephrosis (cortical tubular necrosis), acute, severe, diffuse with intratubular hyaline proteinic casts (consistent with hemoglobinuria) and intracytoplasmic brown to black pigment (consistent with iron/hemosiderin) in proximal tubular epithelial cells.

**Contributor’s Comment:**

The diagnosis of copper poisoning was based on macroscopic and histologic pathological findings which clearly indicated an acute hemolytic crisis coupled with markedly elevated copper concentrations in the kidney and liver. Considering the severity and extension of the lesions, death was attributed to renal and potential hepatic failure.

Copper is a heavy metal and an essential microelement. It acts on cells in different biochemical processes such as respiration, catecholamine biosynthesis, iron metabolism by copper-dependent enzymes, elastin and collagen formation, and melanin production.<sup>12</sup>

Chronic copper poisoning is frequent in sheep, and it has been reported in most sheep rearing regions all over the world.<sup>9</sup> It may occur with daily intakes of 3.5 mg of copper/kg when grazing pastures that contain 15-20 ppm of copper (dry matter).<sup>5</sup> Sheep are particularly susceptible to this condition because they are not able to increase copper biliary excretion as intake increases.<sup>7</sup> Additionally, the protein that aids in the transport of copper in plasma (ceruloplasmin) possess a long half-life in sheep, thus increasing the time this mineral remains in the bloodstream.<sup>4</sup> Although all ovine breeds are susceptible to copper poisoning, Texel sheep (as in this case) are among the most vulnerable.<sup>9</sup>

Chronic copper toxicosis is usually the result of an excessive copper intake for a prolonged

period of time, often associated with contamination of water sources, pasture, or rations.<sup>1</sup> Additionally, secondary factors such as low molybdenum, iron, or sulphate levels in the diet can increase copper absorption and accumulation in the liver. In this case, ingestion of red clover (*Trifolium pratense*) could have predisposed this animal to retain excessive copper as clover can have elevated copper:molybdenum ratios.<sup>5,10</sup> Although molybdenum was not detected in liver and kidney of this sheep, the diet was not tested for molybdenum as would have been required to assess molybdenum intake.

Other factors including the ingestion of hepatotoxic plants such as those containing pyrrolizidine alkaloids (e.g. *Senecio* spp.) can induce copper release from damaged hepatocytes, resulting in increased blood levels of copper and risk of hemolytic crisis.<sup>1,5</sup> To the best of our knowledge, the sheep in this flock were not exposed to hepatotoxic plants. Stress resulting from starvation, vigorous exercise, transportation, handling, and/or adverse weather conditions could elicit the hemolytic crisis typical of copper poisoning.<sup>5</sup>

When toxic quantities of copper are released into the bloodstream, intravascular hemolysis occurs due to a reduction of the antioxidant capacity of erythrocytes and lipid peroxidation of their cell membrane. The resulting hemoglobinemia ultimately leads to hypoxia and hemoglobinuric nephrosis.<sup>6,14</sup>

Carcasses usually exhibit diffuse yellow discoloration (jaundice) of the subcutaneous tissue, fat and mucosae.<sup>1,13</sup> The liver can be enlarged and diffusely ochre/orange due to bile retention.<sup>1,5</sup> The spleen is often enlarged, dark and soft.<sup>1,5</sup> A black or dark red discoloration is present in the kidneys (colloquially referred to as gunmetal kidneys).<sup>5,13</sup> The

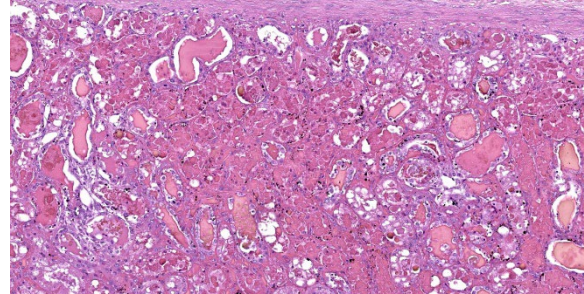


**Figure 3-4. Kidney sheep. Higher magnification of affected tubular lumina, which contain variable amounts of luminal protein and hemoglobin casts. (HE, 147X)**

urine is also dark red, resembling port-wine due to hemoglobinuria.<sup>5,13</sup>

Differential diagnoses for acute jaundice and hemoglobinuria/hemoglobinuric nephrosis in sheep include bacterial diseases such as bacillary hemoglobinuria (*Clostridium haemolyticum*) and eperythrozoonosis (*Mycoplasma ovis*), parasitic diseases such as bovine theileriosis (*Theileria lestoquardi*, *T. uilenbergior* and *T. luwenshuni*) and babesiosis (*Babesia ovis* and *B. motasi*), and plant toxicoses (*Allium cepa* and *Brassica* spp.). In lambs, leptospirosis, yellow lamb disease (*Clostridium perfringens* type A), and type D enterotoxemia (*C. perfringens* type D) should be considered as well.<sup>3,8</sup>

Frequent histological findings of copper poisoning include centrilobular hepatocellular necrosis accompanied by pigment laden Kupffer cells.<sup>6,14</sup> Rhodanine stain can be used to highlight intracellular copper. Portal mixed inflammatory infiltrates are also common.<sup>1,6</sup> Renal lesions usually consist of acute tubular necrosis with intratubular eosinophilic casts.<sup>2,14</sup> The deposition of iron-derived pigments in the cortical tubular epithelial cells, as seen in this case, has not been frequently described in the literature. However, a case presented in a previous Wednesday Slide

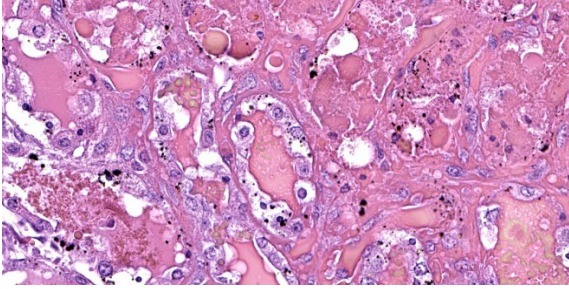


**Figure 3-5. Kidney sheep. Tubular lumina contain abundant protein or hemorrhage/hemoglobin casts. Tubular epithelium is vacuolated and swollen with granular dark brown pigment or is necrotic with granular cytoplasm and sloughs into the lumen. (HE, 555X)**

Conference (Case 1, Conference 14, WSC 2010-2011) also described this finding. In our case, the heavy metal screen revealed that the iron levels in the kidney were markedly elevated, with a less significant elevation in the liver. It is possible that, as intravascular hemolysis progresses, heme iron is released into the plasma, filtered through renal glomeruli and captured by proximal renal tubules eventually leading to histologically visible iron deposits (hemosiderin), which could be highlighted using special stains such as Perl's Prussian blue.

Unequivocal confirmation of copper toxicity requires determination of toxic copper levels in blood ( $>1.5 \mu\text{g/ml}$ ), kidney ( $>15 \text{ ppm}$ , wet weight) and/or liver ( $>250 \text{ ppm}$ , wet weight), although it should be stressed that hepatic levels may decrease after copper is released into the bloodstream during the hemolytic crisis.<sup>5,11</sup>

**Contributing Institution:**

Plataforma de Investigación en Salud Animal, Instituto Nacional de Investigación Agropecuaria (INIA), La Estanzuela, Uruguay.

**JPC Diagnosis:**

1. Liver: Necrosis, centrilobular, diffuse, mild, with cholestasis and intracytoplasmic pigment.
2. Kidney: Tubular degeneration and necrosis, acute, diffuse, severe, with hemoglobin and protein casts.

**JPC Comment:**

The contributor provides an excellent case summary to accompany representative sections from the liver and kidney of this sheep. We agree that the changes in the kidney are severe, though the degree of necrosis within this section of liver is somewhat mild which surprised some participants. Possible explanations include slide/sampling variation as well as the notion that hepatocytes are able to extract oxygen from the portal vein with increasing efficiency during hypoxia. As such, they may be less immediately impacted by loss of erythrocytes/oxygen than the renal tubular epithelial cells supported by the vasa recta.

Conference participants discussed features of copper metabolism (or lack thereof) present within the liver. The large number of bile plugs (canalicular cholestasis) is accompanied by hepatocyte degeneration that is secondary to hypoxia and the growing anemic crisis. Together, these aspects highlight an increase in heme breakdown to biliverdin that is combined with the inability of hepatocytes to secrete bile constituents effectively.

Rhodanine staining highlighted copper within hepatocytes and Kupffer cells, though iron staining was largely unremarkable despite the degree of hemolysis and elevated blood iron concentration in this case, likely attributed to intra- versus extravascular hemolysis. Masson's trichrome showed some bridging fibrosis, though this is an expected and probably

unrelated finding in an aged, grazing sheep, it is possibly indicative of the typical secondary hepatocyte injury, often plant toxicity, that initiates the cascade of hepatocyte death and copper release leading to hemolysis.

The changes in the kidney are classic in this case. We performed a Jones methenamine silver (JMS) and PAS stain to highlight the glomerular and tubular basement membrane – tubulorrhhexis was not a feature of this case, however. We did not identify any copper within the kidney on rhodanine staining. Iron staining highlighted select renal tubular cells described by the contributor as containing hemosiderin; acid hematin is another differential to consider.

#### References:

1. Cullen JM, Stalker M. Liver and Biliary System. In: Maxie MG, ed. *Jubb, Kennedy and Palmer's Pathology of Domestic Animals*. 6th ed., Vol. 2. St. Louis, MO: Elsevier; 2016:258–352.
2. García-Fernández AJ, Motas-Guzmán M, Navas I, María-Mojica P, Romero D. Sunflower meal as cause of chronic copper poisoning in lambs in southeastern Spain. *Can Vet J*. 1999;40:799–801.
3. Giannitti F, Macias-Rioseco M, García JP, et al. Diagnostic exercise: hemolysis and sudden death in lambs. *Vet Pathol*. 2014; 51(3):624–627.
4. Gooneratne SR, Buckley WT, Christensen DA. Review of Copper Deficiency and Metabolism in Ruminants. *Can J Anim Sci*. 1989;69:819–845.
5. Gupta RK. A review of copper poisoning in animals: Sheep, goat and cattle. *Int J Vet Sci Anim Husb*. 2018;3:1–4.
6. Hovda LR. Disorders caused by toxicants. In: Smith BP, ed. *Large Animal Internal Medicine*. 5th ed. St. Louis, MO: Mosby; 2015:1578–1616.
7. López-Alonso M, Prieto F, Miranda M, Castillo C, Hernández J, Benedito JL. The role of metallothionein and zinc in hepatic copper accumulation in cattle. *Vet J*. 2005;169:262–267.
8. Maxie MG. *Jubb, Kennedy and Palmer's Pathology of Domestic Animals*. 6th ed. St. Louis, MO: Elsevier; 2016.
9. McCaughley WJ. Inorganic and Organic Poisons. In: Aitken ID, ed. *Diseases of Sheep*. 4th ed. Oxford, UK: Blackwell Science; 2007:424–439.
10. Millar M, Errington H, Hutchinson JP, Norton A. Copper poisoning in sheep associated with clover. *Vet Rec*. 2007;161:108.
11. Plumlee K. Metals and Minerals. In: *Clinical Veterinary Toxicology*. St. Louis, MO: Mosby; 2004:193–230.
12. Radostits OM, Gay CC, Hinchcliff KW, Constable PD. In: *Veterinary medicine: A textbook of the diseases of cattle, horses, sheep, pigs and goats*. 10th ed. New York, USA: Saunders Elsevier; 2007:1740-1741.
13. Roubies N, Giadinis ND, Polizopoulou Z, Argiroudīs S. A retrospective study of chronic copper poisoning in 79 sheep flocks in Greece (1987-2007). *J Vet Pharmacol Ther*. 2008;31:181–183.
14. Villar D, Pallarés Martínez FJ, Fernández G. Retrospective study of chronic copper poisoning in sheep. *An Vet Murcia*. 2002;60:53–60.

#### CASE IV:

##### **Signalment:**

4-year-old, female, Nevisian Donkey, *Equus asinus*, equine.

##### **History:**

This animal initially presented with a 1-month history of chronic diarrhea and hyporexia. A fecal analysis returned a high





**Figure 4-1. Liver, donkey. There are multifocal to coalescing, white-to-tan nodules that are often depressed and infiltrate the hepatic parenchyma. (Photo courtesy of: Department of Biomedical Sciences, Ross University School of Veterinary Medicine, St. Kitts, West Indies. [www.veterinary.rossu.edu](http://www.veterinary.rossu.edu))**

strongyle count and the animal was subsequently treated for parasites but, there was minimal clinical improvement. An abdominal ultrasound revealed significant peritoneal effusion, an abnormal appearance to the hepatic parenchyma, and an ill-defined mass caudal to the stomach that could not be distinguished as separate from the liver. Hematology, biochemistry, and abdominal fluid analysis was performed - supporting a diagnosis of hepatic disease (see section on laboratory results). Subsequent therapy involved treatment with gentamicin and ceftiofur sodium, which was eventually discontinued when peritoneal fluid analysis was inconsistent with a peritonitis. Heparin therapy was also instituted to treat presumptive hepatic lipidosis. The donkey was found collapsed in sternal recumbency three days later and was euthanized on humane grounds.

#### **Gross Pathology:**

The abdominal cavity contains approximately 9.5 L of light yellow, translucent, low-viscosity fluid. Multiple (~5 mm) pale, firm raised, nodules are present throughout the perito-

neum, mesentery, serosal surfaces of the intestines and on the diaphragmatic surface of the spleen. The majority of the liver contains multifocal to coalescing, firm, white-to-tan, poorly demarcated nodules that measure 0.5-2.5 cm and occasionally have central depressions that are yellow and friable (necrosis). The remainder of the liver is pale yellow, friable, and overall, the liver is enlarged with rounded edges.

There is a large (approximately 20 cm x 10 x 6 cm) multilobulated tan mass in the region of the pancreas along the greater curvature of the stomach. Intra-abdominal lymph nodes are diffusely enlarged and prominent, with multiple nodes having multifocal to coalescing white-yellow lesions expanding the parenchyma with friable, yellow centers (necrosis).

The lungs are diffusely wet and rubbery and have mild rib impressions. Similar nodular lesions to that seen in the abdominal cavity are present in the lungs.

#### **Laboratory Results:**

##### Initial hematology:

Hyperproteinemia (9.0, RI:6.0-8.5g/dL), anemia (PCV 26, RI: 32-48), lymphopenia (0.5, RI: 1.5-5.0 x10<sup>3</sup>/μL), monocytosis (0.9, RI: 0.0-0.6 1.5-5.0 x10<sup>3</sup>/μL)

##### Abdominal fluid analysis:

Total protein 2.4 g/dL

Nucleated cell count: 0.15 x10<sup>3</sup>/μL

Interpretation: Pure transudate

Abdominal fluid culture: aerobic and anaerobic culture yielded no growth.

Biochemistry on the day of euthanasia:

ALP	<b>2261</b>	50.0-170 U/L
ALT	<b>53</b>	5.0-20.0 U/L
GGT	<b>2125</b>	5.0-24.0 U/L
Bile Acids	<b>105</b>	0.0-25.0 μmol/L
TBIL	0.8	0.5-2.4 mg/dL
ALB	3.6	2.2-3.7 g/dL
BUN	9	7.0-25.0 mg/dL
CHOL	<b>155</b>	50.0-140.0 mg/dL
TRIGLYCERIDES	<b>&gt;375</b>	11-68 mg/dL

Fungal culture of the mass yielded no growth.

Aerobic and anaerobic bacterial culture of the mass yielded rare growth of mixed bacteria. Negative for *Nocardia* sp., *Actinomyces* sp. or *Corynebacterium* sp. No anaerobes were isolated

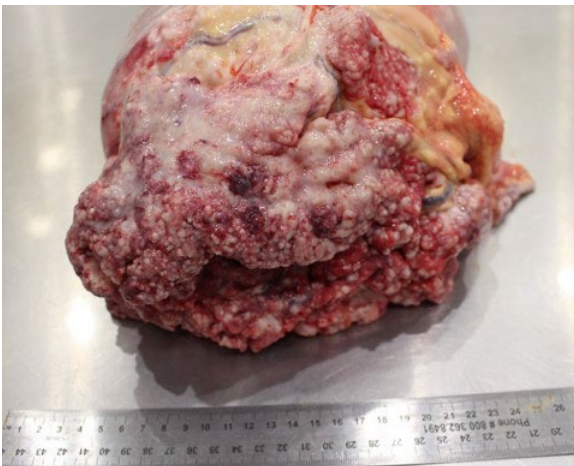


**Figure 4-2. Liver, donkey. There is a multilobular mass in the region of the pancreas along the greater curvature of the stomach. (Photo courtesy of: Department of Biomedical Sciences, Ross University School of Veterinary Medicine, St. Kitts, West Indies. [www.veterinary.rossu.edu](http://www.veterinary.rossu.edu))**

**Microscopic Description:**

Liver: Effacing and replacing over 90% of the examined sections is a poorly demarcated, highly infiltrative, nonencapsulated neoplasm composed of islands of neoplastic epithelial cells forming cords, islands and ducts supported by moderate-to-abundant fibrocollagenous stroma. Neoplastic cells lining ductal structures are predominately columnar with a distinct brush border, variable amounts of pale eosinophilic cytoplasm, and a basilar nucleus with coarse chromatin and up to two small nucleoli. In contrast, neoplastic cells forming cords and islands are often polygonal with larger nuclei closely resembling hepatocytes. Anisocytosis and anisokaryosis are moderate and mitotic figures are rare. Rarely (and not in all sections), seemingly well-differentiated neoplastic hepatocytes appear to transition into neoplastic ductal structures. Within the neoplasm are multiple foci of coagulative necrosis and ducts are frequently filled with sloughed epithelial cells, cellular debris, and eosinophilic secretory material. Thick bands of fibrovascular tissue (scirrhous response) surround and expand the proliferating neoplastic cells and are infiltrated by low numbers of lymphocytes and plasma cells. The remaining, non-neoplastic hepatocytes have shrunken, pale eosinophilic cytoplasm and the hepatic capsule is thickened by fibrous connective tissue and lined by plump mesothelial cells.

Within sections of the pancreas, spleen, lung, and lymph node (not submitted) is a neoplastic process similar to that of the liver.

Immunohistochemistry (IHC): Sections of the mass adjacent to the pancreas and within the liver were labeled for Cytokeratin-19, and Hepar-1. The neoplastic cells forming ductal structures labeled positive with CK19 and mostly negative for Hepar-1. However, in transition zones between neoplastic cells forming cords and resembling hepatocytes

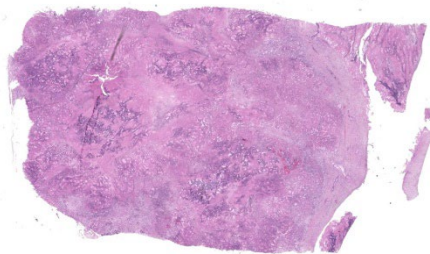


**Figure 4-3. Liver, donkey. In this section of liver, normal hepatic architecture is replaced by a largely necrotic neoplasm. (HE, 5X)**

and neoplastic ducts (presumably biliary) individual cells and clusters of cells in neoplastic ducts also labeled positive with Hepar-1.

**Contributor's Morphologic Diagnosis:**

Liver: Carcinoma (suspect cholangiolocarcinoma)

**Contributor's Comment:**

This case proved particularly challenging due to the extent and size of transcoelomic metastatic spread within the abdomen. The largest mass observed was in the region of the pancreas and this prompted the initial presumptive diagnosis of a pancreatic neoplasm. However, this was later disproven by microscopic examination and immunohistochemistry of the liver which demonstrated rare transitioning of hepatocytes into neoplastic biliary ducts which is more consistent with a hepatic or biliary neoplasm. In either case, both primary hepatic and pancreatic neoplasms are rare in donkeys and horses.<sup>1,2,6</sup>

A retrospective study of post-mortem findings in donkeys with a mean age of 30.6 years (n=1444) from the UK, found that only 4.2% of those examined (60/1444) had malignant liver neoplasms (cholangiosarcoma or bile duct carcinoma) and none had evidence of pancreatic neoplasms.<sup>6</sup> Similar findings

were observed in a survey of donkeys diagnosed with neoplasia (n=125) in which 0.8% (1/125) were diagnosed with a primary hepatic neoplasm (biliary carcinoma) and none had pancreatic neoplasms.<sup>2</sup> Pancreatic adenocarcinoma in donkeys has only been reported twice in the literature with the diagnosis primary based upon location and appearance; no immunohistochemistry was performed in these cases.<sup>3,7</sup>

Classification schemes of primary hepatic tumors are not available for donkeys or horses but have recently been established in canines.<sup>9</sup> In general, primary liver neoplasms are characterized as either hepatocellular, cholangiocellular or neuroendocrine. Mature hepatocytes and cholangiocytes are the proposed origin of primary epithelial liver tumors; however cholangiolocarcinomas are believed to originate from hepatic progenitor cells and have hepatocellular, ductular and cholangiocellular characteristics.<sup>4,9</sup> According to the canine classification scheme, cholangiolocarcinomas differ from cholangiocellular carcinomas morphologically due to the presence of central tubular structures surrounded by solid areas with the appearance of hepatic cords or acini.<sup>9</sup> Furthermore, IHC patterns typical of canine tumors are distinct with tubular structures labelling positive for Keratin-19, EMA/MUC-1 and CD10 while the solid hepatocyte-like areas were positive for Keratin-19 and negative for HepPar-1, EMA/MUC-1 and CD10.

Though not a described entity in donkeys, this case most likely represents a cholangiolocarcinoma or less likely, a cholangiocellular carcinoma.

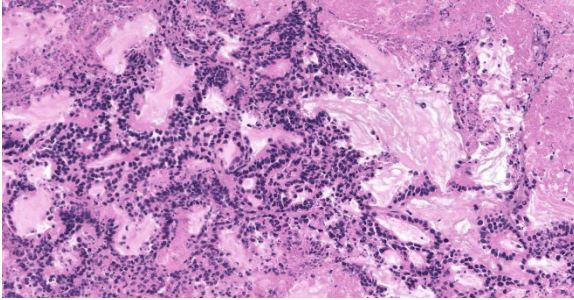


**Figure 4-4. Liver, donkey. Neoplastic epithelium forms tubules within large areas of necrosis. (HE, 314X)**

**Contributing Institution:**

Department of Biomedical Sciences

Ross University School of Veterinary

Medicine, P. O. Box 334; Basseterre, St. Kitts, West Indies

[www.veterinary.rossu.edu](http://www.veterinary.rossu.edu)

**JPC Diagnosis:**

Liver: Cholangiocellular carcinoma.

**JPC Comment:**

The final case of this conference is an interesting neoplasm with several great gross photos. From subgross magnification, conference participants quickly identified invasive behavior and neoplastic spread through the adjacent parenchyma, though evidence of lymphovascular invasion was less definitive. We repeated IHC for HepPar-1, CK7, and CK19 and performed PAS-Alcian Blue and Masson's trichrome stains. IHC results were similar to the contributor – special stains highlighted mucus within neoplastic bile ducts and periductular fibrosis. Based on morphology, we favored a malignant epithelial neoplasm of biliary origin (i.e. cholangiocarcinoma).

The degree of fibrosis (scirrhous response) is fairly mild in this case compared with other

cholangiocarcinomas. Dr. Cullen again highlighted the relationship of biliary epithelium, mesenchyme, and myofibroblasts that was explored in Case 1. Rather than a 'disjointed conversation' leading to inappropriate proliferation of bile ducts and connective tissue as was seen in ductal plate malformation, the phenotype in neoplasia is tilted in favor of collagen fiber deposition with ductular reaction being a minor feature.

Finally, Dr. Cullen weighed in on the idea of a cholangiolocarcinoma for this case. As the contributor hints at, exact definitions of this rare neoplasm are hard to come by with few published cases – as such, readers may benefit from a quick review of Komuta et al<sup>4</sup> which has some excellent figures. MacSween's Pathology of the Liver (a veritable grail of hepatology) itself lacks a definition. Recently published human cases each differed in their microscopic descriptions of the tumor as well.<sup>5,7</sup> The use of IHC is potentially chal-

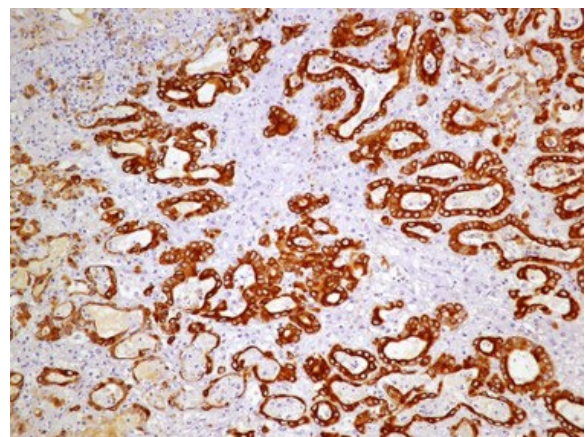


**Figure 4-5. Liver, donkey. Immunohistochemical staining for CK19 demonstrates immunopositivity within the cytoplasm of neoplastic cells with ductal morphology. (anti-cytokeratin 19, 400X) (Photo courtesy of: Department of Biomedical Sciences, Ross University School of Veterinary Medicine, St. Kitts, West Indies. [www.veterinary.rossu.edu](http://www.veterinary.rossu.edu))**

lenging as ruling out metastatic adenocarcinoma may be complicated by lack of complete specificity. For example, many duct forming epithelia, as well as salivary epithelium may react with CK7 and select GI epithelial cells may be positive for HepPar-1. Hepatic progenitor cells may also variably express chromogranin A, similar to a biliary carcinoid. As such, we felt most confident that the neoplasm in this case had features supportive of a cholangiocarcinoma on H&E without IHCs to refute this interpretation.

### References:

1. Beeler-Marfisi J, Arroyo L, Caswell JL, Delay J, Bienzle D. Equine primary liver tumors: A case series and review of the literature. *J Vet Diag Invest.* 2010;22:174–183.
2. Davis CR, Valentine BA, Gordon E, et al. Neoplasia in 125 donkeys (*Equus asinus*): literature review and a survey of five veterinary schools in the United States and Canada. *J Vet Diag Invest.* 2016;28:662–670.
3. Kerr OM, Pearson GR, Rice DA. Pancreatic adenocarcinoma in a donkey. *Equine Vet J.* 1982;14:338–339.
4. Komuta M, Spee B, Borght S, Vander, et al. Clinicopathological study on cholangiolocellular carcinoma suggesting hepatic progenitor cell origin. *Hepatology.* 2008;47:1544–1556.
5. Makino K, Ishii T, Takeda H, et al. Integrated analyses of the genetic and clinicopathological features of cholangiolocarcinoma: cholangiolocarcinoma may be characterized by mismatch-repair deficiency. *J Pathol.* 2024 May;263(1):32-46.
6. Morrow LD, Smith KC, Piercy RJ, et al. Retrospective Analysis of Post-Mortem Findings in 1,444 Aged Donkeys. *J Comp Pathol.* 2011;144:145–156.
7. Sato N, Yamamura K, Oda E, et al. Cholangiolocarcinoma With Multiple Recurrences Successfully Treated With Repeated Liver Resection and Radiofrequency Ablation. *Anticancer Res.* 2020 Dec;40(12):7147-7153.
8. Spanton JA, Mair TS, Krudewig C. Pancreatic adenocarcinoma in a donkey. Use of laparoscopy to aid the diagnosis. *Equine Vet Educ.* 2009;21:19–24.
9. Van Sprundel RGHM, Van den Ingh TSGAM, Guscetti F, et al. Classification of primary hepatic tumours in the dog. *Vet J.* 2013;197:596–606.